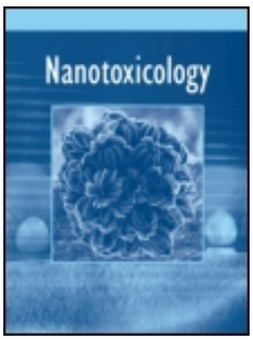

Nanotoxicology

ISSN: 1743-5390 (Print) 1743-5404 (Online) Journal homepage: https://www.tandfonline.com/loi/inan20

Exploring the aneugenic and clastogenic potential in the nanosize range: A549 human lung carcinoma cells and amorphous monodisperse silica nanoparticles as models

Laetitia Gonzalez, Leen C. J. Thomassen, Gina Plas, Virginie Rabolli, Dorota Napierska, Ilse Decordier, Mathieu Roelants, Peter H. Hoet, Christine E. A. Kirschhock, Johan A. Martens, Dominique Lison & Micheline Kirsch-Volders

To cite this article: Laetitia Gonzalez, Leen C. J. Thomassen, Gina Plas, Virginie Rabolli, Dorota Napierska, Ilse Decordier, Mathieu Roelants, Peter H. Hoet, Christine E. A. Kirschhock, Johan A. Martens, Dominique Lison & Micheline Kirsch-Volders (2010) Exploring the aneugenic and clastogenic potential in the nanosize range: A549 human lung carcinoma cells and amorphous monodisperse silica nanoparticles as models, Nanotoxicology, 4:4, 382-395, DOI: 10.3109/17435390.2010.501913

To link to this article: https://doi.org/10.3109/17435390.2010.501913

Nanotoxicology, December 2010; 4(4): 382–395

informa
healthcare

Exploring the aneugenic and clastogenic potential in the nanosize range: A549 human lung carcinoma cells and amorphous monodisperse silica nanoparticles as models

LAETITIA GONZALEZ[1], LEEN C. J. THOMASSEN[2], GINA PLAS[1], VIRGINIE RABOLLI[3], DOROTA NAPIERSKA[4], ILSE DECORDIER[1], MATHIEU ROELANTS[5], PETER H. HOET[4], CHRISTINE E. A. KIRSCHHOCK[2], JOHAN A. MARTENS[2], DOMINIQUE LISON[3], & MICHELINE KIRSCH-VOLDERS[1]

[1]*Laboratory of Cell Genetics, Department of Biology, Vrije Universiteit Brussel, Brussels,* [2]*Center for Surface Chemistry and Catalysis, Katholieke Universiteit Leuven, Heverlee,* [3]*Louvain Center for Toxicology and Applied Pharmacology, Université catholique de Louvain, Brussels,* [4]*Laboratory of Lung Toxicology, Katholieke Universiteit Leuven, and* [5]*Laboratory of Anthropogenetics, Department of Biology, Vrije Universiteit Brussel, Brussels, Belgium*

(Received 29 December 2009; accepted 10 June 2010)

Abstract
We explored how to assess the genotoxic potential of nanosize particles with a well validated assay, the *in vitro* cytochalasin-B micronucleus assay, detecting both clastogens and aneugens. Monodisperse Stöber amorphous silica nanoparticles (SNPs) of three different sizes (16, 60 and 104 nm) and A549 lung carcinoma cells were selected as models. Cellular uptake of silica was monitored by ICP-MS. At non-cytotoxic doses the smallest particles showed a slightly higher fold induction of micronuclei (MNBN). When considering the three SNPs together, particle number and total surface area appeared to account for MNBN induction as they both correlated significantly with the amplitude of the effect. Using nominal or cellular dose did not show statistically significant differences. Likewise, alkaline comet assay and FISH-centromeric probing of MNBN indicated a weak and not statistically significant induction of oxidative DNA damage, chromosome breakage and chromosome loss. This line of investigation will contribute to adequately design and interpret nanogenotoxicity assays.

Keywords: *Amorphous silica nanoparticles, genotoxicity, aneuploidy, dosimetry, size*

Introduction

The genotoxic potential of a broad array of nanoparticle types (chemical composition, form, size etc.) has already been explored, mainly by assessing DNA damage, but without reaching clear conclusions, in part because of the absence of appropriate methodological guidelines (Gonzalez et al. 2008; Landsiedel et al. 2009). Assessing the genotoxicity of nanoparticles (NPs) requires a re-evaluation of the testing procedure, at least for five major reasons: (i) The nanosize range implies physico-chemical interactions more probably driven by laws of quantum physics than by those of classic physics; (ii) the size-dependent behaviour of NP in suspension is driven by gravity, diffusion and convection forces (Teeguarden et al. 2007; Lison et al. 2008); (iii) their cellular uptake kinetics may vary with size (Zhang and Monteiro-Riviere 2009); (iv) the smallest NPs are in the same size range as some important sub-cellular structures (microtubules (25 nm in diameter), the actin filaments (7 nm in diameter), centrosomes (the γ-tubulin ring complex with a diameter of 25 nm); and (v) their mode of action, potentially different from their micro-size equivalents. Assessing all these events is of primary importance because it is known that both clastogenic and aneugenic effects can act as driving forces in the acquisition of a malignant phenotype (Dey 2004; Kops et al. 2005).

To explore how to more adequately assess the genotoxic potential of NPs, we selected well-characterized, monodisperse, insoluble, amorphous SNPs and the A549 human lung carcinoma cell line as models. Amorphous SNPs were chosen

Correspondence: Laetitia Gonzalez, Laboratory of Cell Genetics, Vrije Universiteit Brussel, Pleinlaan 2, 1050 Brussels, Belgium. Tel: +32 2629 3149, Fax: +32 2629 2759. E-mail: lgonzale@vub.ac.be

ISSN 1743-5390 print/ISSN 1743-5404 online © 2010 Informa UK, Ltd.
DOI: 10.3109/17435390.2010.501913

because their micrometer counterparts are generally considered relatively inert (International Agency for Research on Cancer [IARC] monograph Vol. 68, 1997; Merget et al. 2002), enabling us to investigate the potential genotoxic effects mainly due to the nanosize. Furthermore, SNPs are insoluble, their synthesis is tunable with relative ease at the nanoscale, cellular dose can be measured conveniently and they are relevant for many industrial applications.

A549 epithelial lung carcinoma cells were selected because they represent a relevant cell type/tissue for the most probable route of exposure, i.e., inhalation. Moreover this cell line is p53- and caspase 3-proficient, favouring a functional DNA damage and apoptotic response, and is therefore adequate to avoid irrelevant *in vitro* genotoxic responses that would not be confirmed *in vivo*. It has also been reported that SNPs can penetrate A549 cells, but remain outside the nuclear region (Jin et al. 2007).

Until now there is no evidence for the induction of genotoxic effects by amorphous SNPs. Treatment of A549 human lung epithelial carcinoma cells with 50 nm SNPs and 3T3-L1 fibroblasts with amorphous SNPs of varying sizes (20–240 nm) showed no induction of oxidative DNA damage, as assessed by the alkaline comet assay (Jin et al. 2007; Barnes et al. 2008). In contrast, crystalline SNPs were shown to induce genotoxic events. Yang et al. (2009) showed the induction of oxidative DNA damage by 20 nm crystalline SNPs in primary mouse embryo fibroblasts (Yang et al. 2009). Wang et al. (2007b) demonstrated an increase in micronuclei and mutations frequency after exposure of the WIL2-NS human B cell lymphoblastoid cell line to 7.2 nm crystalline SNPs. Remarkably, alkaline comet analysis revealed no oxidative DNA damage (Wang et al. 2007b). Considering the criteria proposed by Gonzalez et al. (2008) these studies present, however, shortcomings, predominantly in the physico-chemical characterization of the tested materials and because of the lack of replicates and/or repeat experiments. Moreover these studies focused essentially on one potential mechanism by which nanomaterials could induce genotoxicity, i.e., the generation of reactive oxygen species (ROS). Therefore these data on the potential genotoxicity of SNPs should be considered with caution, and more systematic approaches assessing the genotoxicity with validated or new assays, optimized for NP testing, covering additional genotoxicity endpoints are needed (Gonzalez et al. 2008).

We studied here a set of three well characterized SNPs (16, 60 and 104 nm) (Thomassen et al. 2010) with the alkaline comet assay (with and without formadidopyrimidine DNA glycosylase, FPG) and a well validated assay, the *in vitro* cytochalasin-B micronucleus assay (CBMN) alone or in combination with FISH-centromeric staining, allowing the detection of DNA/chromosome breaks as well as aneugenic events. As long as tests are not fully validated for nanomaterials it is, indeed, compulsory in this exploratory phase to apply in parallel several complementary approaches with different specificities and sensitivities. The study was purposely conducted at non-cytotoxic doses of SNPs in order to focus on primary genotoxic mechanisms. Mass, particle number and surface area doses, both as nominal or cell-associated doses, were considered as possible determinants of genotoxicity. In addition, two main modes of action, i.e., generation of reactive oxygen species (ROS) and mechanical interference with the cell division machinery, were investigated.

Materials and methods

Stöber silica nanoparticles

Amorphous Stöber SNPs with three different diameters 16.4 nm (S-16), 60.4 nm (S-60) and 104 nm (S-104) were used. The main characteristics of these monodisperse particle suspensions are given in Table I. Method of synthesis and physico-chemical characterization have been published previously (Thomassen et al. 2010). Dynamic light scattering (DLS; ALV high performance particle sizer) measurements were performed to measure the hydrodynamic diameter of the particle suspensions at 37°C in complete DMEM medium (with 10% FCS). DLS measurements were performed on particle suspensions of S-16 (concentrations of 10–60 μg/ml), S-60 (concentrations of 10–60 μg/ml) and S-104 (concentrations of 40–300 μg/ml), corresponding to the concentrations used in the genotoxicity assays. The scattering was measured at an angle of 173° to the incident He/Ne laser beam (632.8 nm, 3 mW power).

Cell culture

The A549 human lung carcinoma cell line (p53 and caspase-3 proficient) was obtained from the American Type Culture Collection (ATCC, Manassas, USA [CCL-185]). Cells were cultured in Dulbecco's Modified Eagle Medium (DMEM) supplemented with 10% fetal calf serum (FCS), 1% penicillin/streptomycin and 1% sodium pyruvate (Gibco, Merelbeke, Belgium). Cells were maintained in a humidified atmosphere of 5% CO_2 at 37°C. All experiments were performed in the same culture conditions on exponentially growing cultures.

Table I. Main physico-chemical characteristics of monodisperse, amorphous silica nanoparticles.

Particle	Particle size* (nm)	Specific external surface area (m^2/g)	Aggregation status in complete DMEM medium	Zeta potential in complete DMEM medium (mV)	ED_{50} (μg/ml)
S-16	16.4 ± 2.5	183	No particle-particle aggregation but particle-protein interactions/flocculation	−13	45.9
S-60	60.4 ± 8.3	33	No aggregation up to 7 days	−13	48.9
S-104	104 ± 9.9	28	No aggregation up to 7days	4	165.3

Particle size, specific surface area, aggregation status in complete DMEM medium (DMEM medium supplemented with 10% FCS and 1% penicillin/streptomycin), zeta potential in complete DMEM medium and ED_{50} values measured are given. Particle size distribution was determined by SEM/TEM. The specific surface area was determined by nitrogen adsorption at −196°C. Isotherms were interpreted by the α_s-method. Particle aggregation was analyzed by DLS. Measurements of the zeta potential were performed on a BIC ZetaPALS (Brookhaven Instruments Corp.) in DMEM. The dose at which 50% cytotoxicity is induced in A549 cells (ED_{50}) was determined by the MTT (3-(4,5-dimethylthiazol-2-yl)-2,5-diphenyltetrazolium bromide) assay after 24 h of exposure. *Arithmetic mean ± SD.

Tetrazolium salt (MTT) assay

Cells were seeded in flat-bottomed 96-well plates with a density of 10,000 cells per well. Treatment with freshly prepared SNP suspensions (dilution of stock suspensions in complete medium) was performed 24 h after seeding at concentrations of 10–500 μg/ml. After 24 h treatment with SNP suspensions (in absence of FCS), cells were incubated for 4 h with 3-(4,5-dimethylthiazol-2-yl)-2,5-diphenyltetrazolium bromide (MTT). The formazan product was dissolved in 10% SDS/0.01M HCl solution. Absorbance was recorded at a wavelength of 595 nm and a reference wavelength of 655 nm. Results were calculated as percentages of the untreated control values.

The in vitro cytochalasin-B micronucleus (CBMN) assay

The CBMN assay was performed according to the draft Organization for Economic Co-operation and Development guideline 487 (OECD 2008). Cells were seeded in flat-bottomed 96-well plates with a density of 10,000 cells per well. Treatment with freshly prepared SNP suspensions (dilution of stock suspensions in complete medium) was performed 24 h after seeding. Concentrations were chosen based on previously published cytotoxicity results with these SNPs (Lison et al. 2008; Napierska et al. 2009). A549 cells were treated with doses of 10–60 μg/ml and 40–300 μg/ml of the 16 nm, 60 nm and 104 nm SNPs, respectively, during 40 h, corresponding to less than 2 cell cycles (cell cycle = 22 hours). Tungsten carbide-cobalt (100 μg/ml) was used as a positive control (De Boeck et al. 2003). After 4 h of treatment, 2.5 μg cytochalasin-B/ml was added to the cultures. This time point was chosen to avoid potential interaction of cytochalasin-B with the uptake of the SNPs. After treatment, cells were detached by trypsin/EDTA-treatment (Gibco, Merelbeke, Belgium) and collected. Cells were cytospinned onto microscopic slides and fixed in 100% methanol. Samples were stained with 5% Giemsa (Merck, Darmstadt, Germany) in Sorensen buffer (pH 6.8) (Prosan, Gent, Belgium) for 20 min. Blinded scoring of the slides was performed under a light microscope (Olympus magnification 500×) using the criteria for micronucleus scoring as determined by the International Collaborative Project on Micronucleus Frequency in Human Populations (HUMN project) (Fenech et al. 2003). Two independent experiments were performed. For each experiment two cultures were scored and at least 500 binucleated cells were scored for every culture. Different parameters were recorded: % binucleates, % polynucleates, ‰ binucleates with micronuclei (MNBN) and ‰ mononucleates with micronuclei (MNMONO). MNBN reflect chromosome breakage and loss occurring during the last mitosis in culture. MNMONO are indicators of aneugenic effects resulting from mitotic slippage (Elhajouji et al. 1998) and their assessment was recommended in the OECD guideline. The mitotic index was scored and the cytokinesis-block proliferation index (CBPI) was calculated with the following formula:

$$\text{CBPI} = (\text{number mononucleate cells} + 2 \times \text{number binucleate cells} + 3 \times \text{number multinucleate cells})/\text{total number of cells (Kirsch-Volders et al. 2003, 2004)}$$

For each experiment fold increases of micronuclei (MN) in mononucleated and binucleated cells were calculated by dividing mean MN frequencies of the treated cultures by mean MN frequencies of untreated cultures.

Measurements of cell-associated silica

Cells were seeded (24-well plates) with a density of 60,000 cells per well; 24 hours after seeding, A549 cells were treated with 16 nm (10–60 μg/ml), 60 nm (10–60 μg/ml) and 104 nm SNPs (40–300 μg/ml) for 24 h. After incubation with SNPs, the cells were washed twice in PBS and solubilized in MilliQ water containing 0.1% Triton X100 before direct silicon measurement by inductively coupled plasma mass spectrometry (Agilent 7500) using a certified silicon solution as standard. The results were expressed in μg SiO_2 per ml, corresponding to the content of one culture well.

Alkaline comet assay

Cells were seeded in flat-bottomed 96-well plates with a density of 10,000 cells per well; 24 h after seeding, cells were treated during 15 min and 4 h with 16 and 60 nm SNPs at concentrations of 40 and 60 μg/ml. H_2O_2 (100 μM), a known oxidative damaging agent, was used as positive control in the alkaline comet assay (Decordier et al. 2007). The alkaline comet assay was performed as described previously with minor modifications (De Boeck et al. 1998). Briefly, after trypsinization, cells were mixed with 300 μl of low melting point agarose (0.8% w/v in PBS) and loaded onto a normal pre-coated microscopic slide (normal melting point agarose 1% w/v in water). After lysis at 4°C (2.5 M NaCl, 100 mM NA_2EDTA, 10 mM Tris supplemented with 1% Triton-X100 and 10% DMSO just before use), slides were rinsed twice with enzyme buffer (40 mM HEPES, 100 mM KCl, 0.5 mM EDTA, 0.2 mg/ml BSA; pH 8) prior to incubation with 75 μl formadidopyrimidine DNA glycosylase (FPG; New England Biolabs, Leusden, The Netherlands) for 35 min at 37°C. FPG was chosen because of the great efforts that recently have been made by the European Comet Validation Group (ECVAG) to validate this method (Johansson et al. 2010, Møller et al. 2010). Furthermore 8-oxo-2′-deoxyguanosine (8-oxo-dG) is the most common oxidative lesion (Pluskota-Karwatka 2008). Potential interaction of SNPs with the FPG enzyme was checked. Unwinding of the DNA was performed in a buffer containing 300 mM NaOH and 1 mM Na_2EDTA (pH > 13) for 40 min at 17°C. Alkaline electrophoresis was performed in the same buffer for 20 min at 0.7 V/cm (25 V, 300 mA). The slides were then rinsed three times for 5 min each with 0.4 M Tris (pH 7.5) and dehydrated in ice-cold absolute ethanol for 10 min. Prior to analysis, the slides were rehydrated with deionized water (200 μl, 10 min) and stained with ethidium bromide (20 μg/ml, 10 min). Two independent experiments were performed. Fifty randomly chosen, non-overlapping comets per coded slide (2 slides/treatment point) were captured using a Leitz fluorescence microscope (25× objective) coupled to a CCD camera and an image analysis system (Komet 3.0; Kinetic Imaging Ltd, Liverpool, UK). Percentage of tail DNA (TD) was recorded as DNA damage parameter.

Fluorescence in situ hybridization (FISH)

Cells were seeded 24-well plates with a density of 60 000 cells per well; 24 h after seeding A549 cells were treated for 40 h with 16 nm and 60 nm SNPs at concentrations of 40 and 60 μg/ml. Nocodazole (0.02 μg/ml), a potent aneugen, was chosen as a positive control (Elhajouji et al. 1997). This second series of CBMN assay experiments was performed under the same experimental conditions with a modification of the fixation step to allow FISH. After cold hypotonic treatment (110 mM KCl), cells were fixed three times with a methanol: acetic acid mixture (3:1). Fixed cells were spread on microscope slides, air-dried and stored at −20°C.

FISH was performed as described previously by Elhajouji et al. (1997) and Muller et al. (2008). MN frequencies were scored in ± 500 cytochalasin-B blocked binucleated cells (CB) per culture and per concentration, with a maximum of 1000 CB per culture. The same scoring criteria described previously for the MN assay were applied. In CBs approximately 50 MN were examined per concentration for the presence of one or more spots and were classified as centromere-positive (C+ MN) or centromere-negative (C− MN). The preparations were examined with a Zeiss Axioscop microscope (Carl Zeiss) equipped with a triple bandpass filter no. 25 (Zeiss) to visualize the FITC-labelled probe and the propidium iodide counterstaining at a magnification of 630×.

Statistics

Treatment-related differences were evaluated for each SNP using one-way analysis of variance (ANOVA) followed by pairwise comparisons using the Student-Newman-Keuls post-hoc test (Hoppe 1993). The effect of dose metrics and particle type on the induction of MNBN was analyzed with simple and multiple linear regression analyses on the set of data obtained with all the SNPs. The statistical analysis was performed with SPSS for Windows, Rel. 16 (SPSS Inc.

Chicago, USA). Statistical significance was considered at $p < 0.05$.

Results

Stöber silica nanoparticles

Amorphous Stöber SNPs with three different diameters 16.4 nm (S-16), 60.4 nm (S-60) and 104 nm (S-104) were synthesized and characterized. Method of synthesis and physico-chemical characterization have been published previously (Thomassen et al. 2010). The main characteristics of these monodisperse particle suspensions are given in Table I. Dynamic light scattering (DLS) measurements were performed to assess the hydrodynamic diameter of the particles in culture conditions, i.e., at 37°C in complete DMEM medium (with 10% FCS) (Figure 1). The formation of particles with a hydrodynamic diameter around 100 nm for the three tested SNPs is most probably indicating protein binding to the SNPs. A second population at smaller hydrodynamic diameter (3–10 nm) indicates the abundant presence of serum proteins.

Response to SNPs in the in vitro cytochalasin-B micronucleus assay

To investigate the response to SNPs and to assess the effect of size within the nano-range, the genotoxic potential of the three amorphous SNPs (16, 60 and 104 nm) was first investigated with the *in vitro* cytochalasin-B micronucleus assay (CBMN assay). Doses were chosen based on cytotoxicity data obtained for A549 cells with the MTT assay. The doses leading to a 50% reduction of MTT activity (ED_{50}) are given in Table I.

At the time point when the MN frequencies were assessed (40 h) and under the same conditions (in presence of FCS), the cell proliferation was evaluated by the cytokinesis-block proliferation index (CBPI) based on nuclearity. No statistically significant decrease in cell proliferation was observed after treatment with 16 nm, 60 nm or 104 nm SNPs (Supplementary Figure 1, available online).

The MNBN frequencies induced by 16, 60 and 104 nm SNPs are given in Figure 2. The data are presented as fold induction of MNBN as a function of the mass dose of SNPs (Figure 2, panel A). Treatment with 100 μg/ml WC-Co induced a 1.5-fold increase in MNBN. A maximum fold increase in MNBN of 1.8, 1.4 and 1.4 compared to untreated controls was induced by 16, 60 and 104 nm SNPs, respectively. These increases were not statistically significant but the smallest SNPs appeared to induce more MNBN. No clear dose-effect relationship was apparent when considering mass dose.

In parallel with the scoring of MN in binucleated cells, MN were scored in mononucleated cells (MNMONO). MNMONO represent the background frequency of MN, cells that did not divide or cells that divided but escaped cytokinesis-block. In the CBMN assay an increase of MN in mononucleated (MNMONO) cells provides an indication for mitotic slippage (Kirsch-Volders and Fenech 2001). Cells blocked in metaphase can progress untimely into the following interphase, without undergoing chromatid segregation and cytokinesis. This abnormal mitotic exit, also called mitotic slippage, is caused by the early degradation of maturation promoting factor (MPF) and yields 4N, 4C cells (Elhajouji et al. 1998; Decordier et al. 2008). Results show that some mitotic slippage was observed with the tested SNPs, although increases were not statistically significant (Figure 3).

These data indicate that: (i) SNPs do not induce a significant increase of MNBN at sub-cytotoxic concentrations, (ii) when considering mass dose, the smallest SNPs appear to elicit a slightly higher fold MNBN induction, and (iii) some induction of MNMONO, possibly reflecting some mitotic slippage, was observed.

Dose-effect and dose-response relationships

The assessment of the (geno-)toxic activity of a test compound usually relies on the demonstration of two main elements: (i) A statistically significant excess of abnormal events against untreated controls, and/or (ii) a significant dose-effect or dose-response relationship. Exploring the latter with NPs has been hampered by the difficulty to define the appropriate dose metrics, which has been heavily debated in the field of nanotoxicology (Oberdörster et al. 2007; Stoeger et al. 2007; Wittmaack 2007). To explore the most appropriate dose metric for genotoxic effects of SNP, we also expressed the data as a function of particle number and surface area doses, as shown in Figures 2B and 2C. Linear regression analysis was performed on the MNBN data of the three SNPs. When considering the three SNPs together, MNBN induction correlated in a statistically significant way with the nominal particle number ($p < 0.001$) and total surface area ($p = 0.041$), but not with the nominal mass dose ($p = 0.598$). These results suggest that the particle number and total surface area could determine *in vitro* MNBN induction by SNPs.

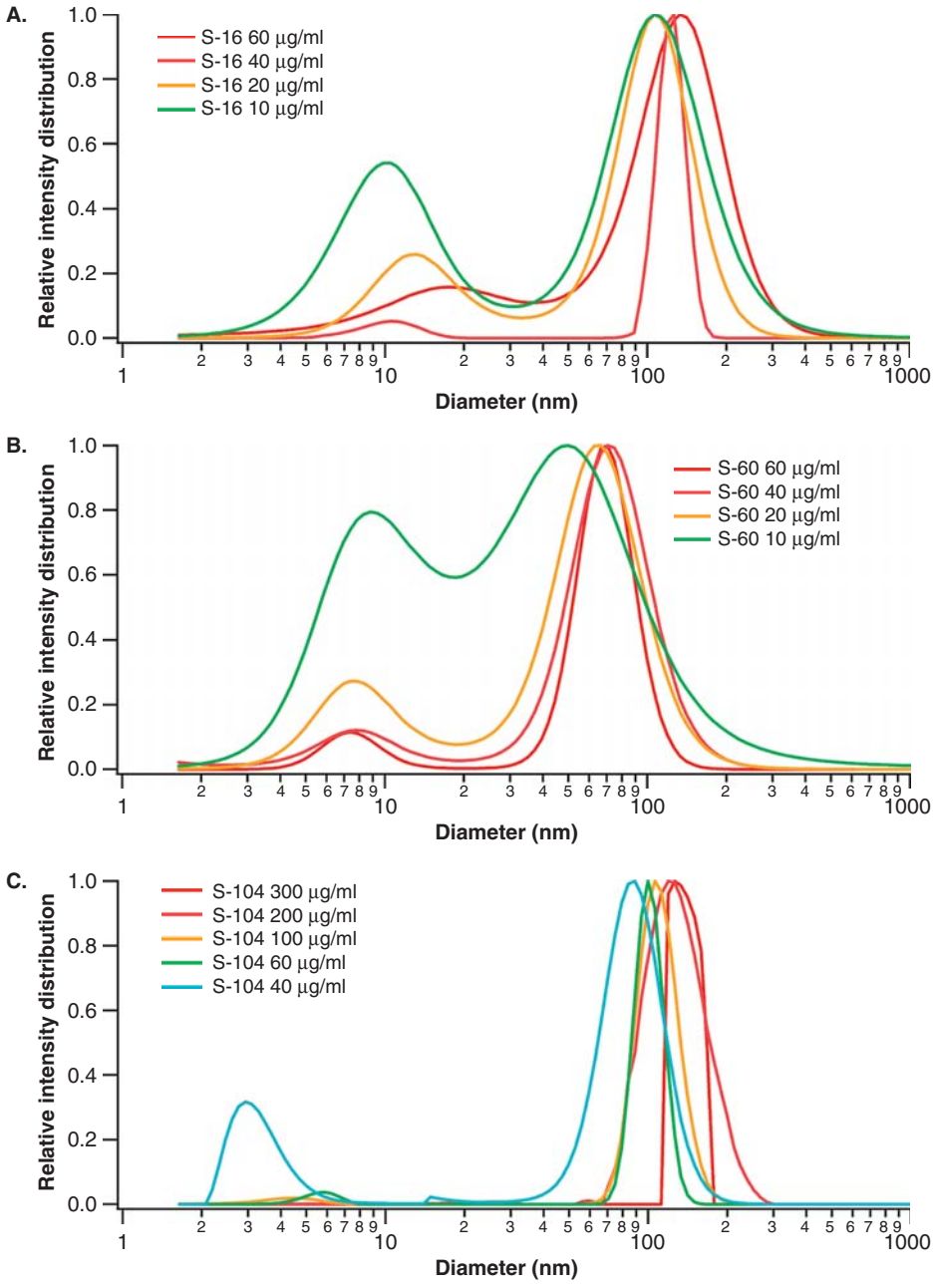

Figure 1. DLS measurements performed at 37°C and in complete DMEM medium for the S-16 (A), S-60 (B) and S-104 (C).

Nominal versus cellular dose

It was previously shown by us that when considering cytotoxicity assays with SNPs, the nominal dose was an appropriate metric to assess dose-effect relationships (Lison et al. 2008). Since targets for genotoxicity are by definition intracellular, the cellular dose might, however, be more adequate to assess genotoxic dose-effect/response relationships. Therefore, a quantification of the cellular dose (cell-associated silica) was performed at time points from 15 min (data not shown) to 40 h (Figure 4A) after exposure. Already after 15 min a small fraction (on average 0.23% S-16, 0.21% S-60 and 0.19% S-104) of SNPs was found associated with the cells. At the time point when MNBN were assessed (40 h, Figure 4A) a relatively low but dose-dependent increase of cell-associated silica was found. The amount of cell-associated silica was higher after treatment with 60 nm SNPs in comparison with 16 nm SNPs. Treatment with 104 nm SNPs resulted in a markedly lower amount of cell-associated silica (0.01% after 40 h). The frequencies of MNBN were plotted against the cell-associated mass (Figure 4, panel B), particle number (Figure 4, panel C) or

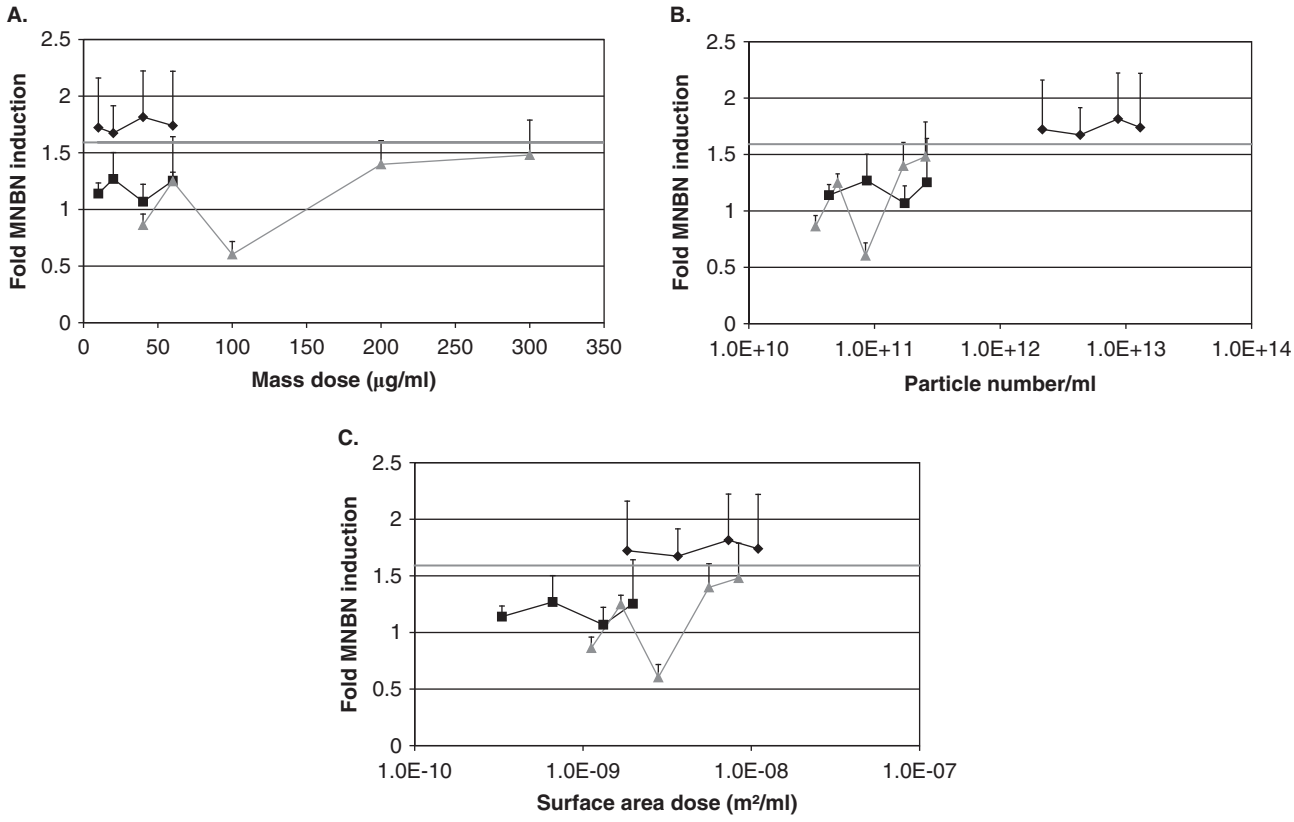

Figure 2. Fold MNBN induction as compared to untreated controls as function of nominal (A) mass, (B) particle number and (C) external surface area dose after 40 h treatment of A549 cells with 16 (◇), 60 (■) and 104 (▲) nm SNPs. The values represent the mean of two experiments ± SEM. For each experiment at least two replicates were performed. The fold MNCB induced by 100 µg/ml WC-Co, the positive control, is indicated by the grey line (—). No statistically significant difference was observed by one-way ANOVA. Linear regression analysis demonstrated a statistically significant relationship between MNBN induction and particle number ($p = 0.000$) and MNBN induction and surface area dose ($p = 0.041$).

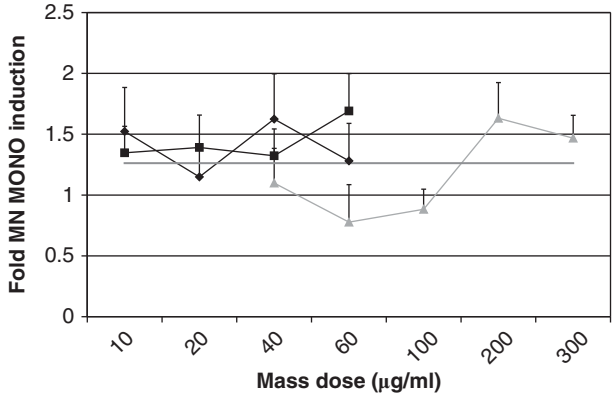

Figure 3. Fold induction of MN in mononucleated cells (MNMONO) after 40 h treatment of A549 cells with 16 nm (◇), 60 nm (■) and 104 nm (▲) SNPs compared to untreated control values. The values represent the mean of two experiments ± SEM. For each experiment at least two replicates were performed. The fold MNCB induced by 100 µg/ml WC-Co, the positive control, is indicated by the grey line (—). The average untreated control value is 23.57 ± 2.99 MNMONO/1000 cells. No statistically significant difference between mean values measured in the indicated groups compared to untreated control were observed by one-way ANOVA.

surface area dose of SNPs (Figure 4, panel D). The fold MNBN induction as a function of the cell-associated mass dose (Figure 4, panel B) indicated that the mass of SNPs associated to the cells is apparently not a better parameter than nominal mass dose to account for MN induction. Considering all tested SNPs together, linear regression analysis demonstrated a statistically significant correlation of fold MNBN induction with cell-associated particle number ($p = 0.024$) and cell-associated surface area ($p = 0.025$) but not with cellular mass dose ($p = 0.302$). As for the nominal doses, it was, however, not possible to discriminate between the influence of surface area or particle number dose and that of SNP type (16, 60 or 104 nm) in a multiple linear regression analysis (data not shown).

In vitro induction of DNA strand breaks and oxidized purines

Since, until now, the generation of reactive oxygen species (ROS) has been considered as the main

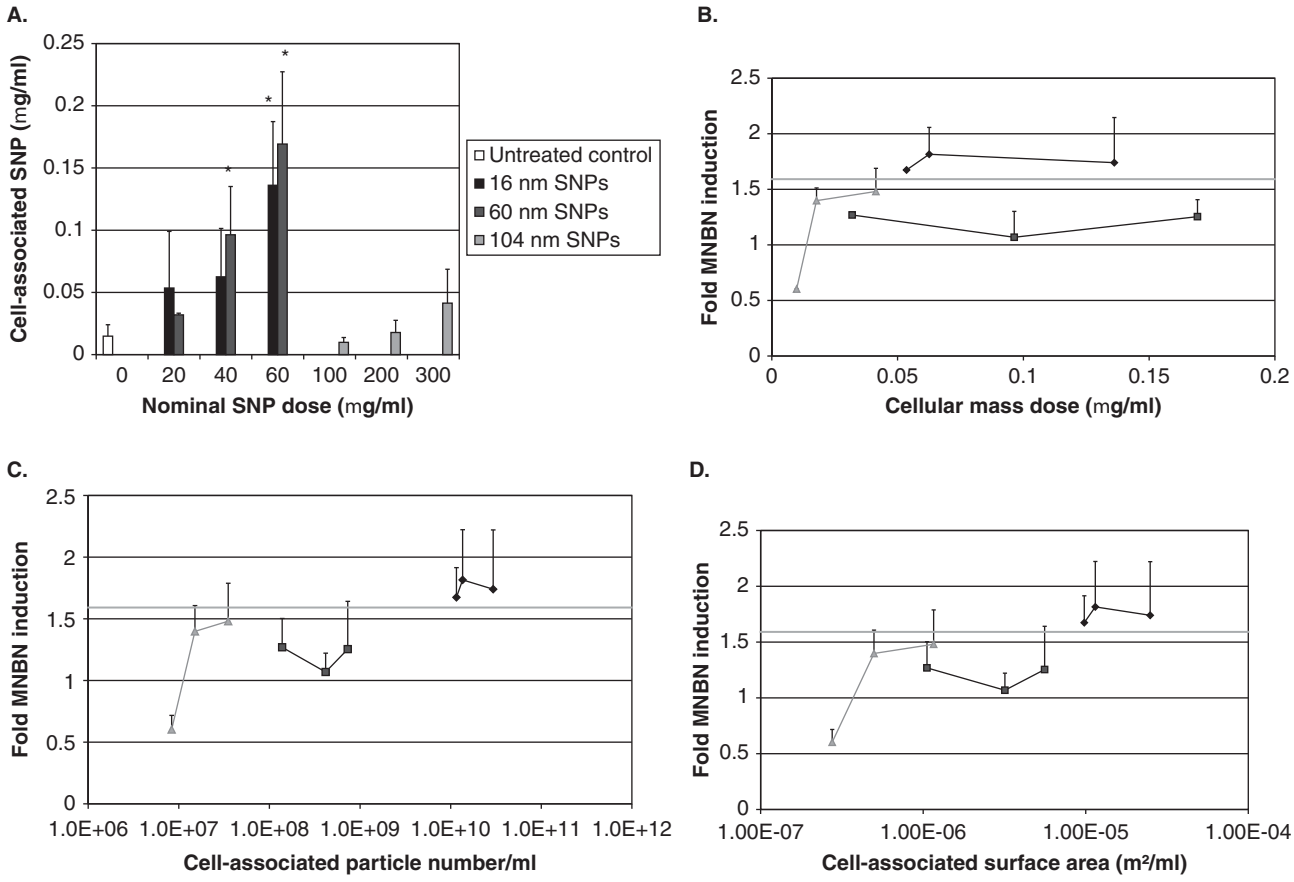

Figure 4. The amount of cell-associated SiO_2 as function of the nominal mass dose of SiO_2 – nanoparticles in suspension (panel A) and fold induction of MNBN as function of the cellular mass dose (B) 40 h after treatment with 16 (◊), 60 (■) and 104 (▲) nm SNPs. The fold induction of MNBN was also expressed as function of cell-associated particle number/ml (C) and surface area/ml (D). The values represent the mean of two experiments ± SD (panel A) or SEM (panel B, C, D). The fold MNCB induced by 100 μg/ml WC-Co, the positive control, is indicated by the grey line (——). For each experiment at least two replicates were performed. *denotes a statistically significant difference ($p < 0.05$) compared to untreated controls as assessed by ANOVA and Student-Newman-Keuls post-hoc test. Linear regression analysis demonstrated a statistically significant relationship between MNBN induction and cell-associated particle number ($p = 0.024$) and MNBN induction and cell-associated surface area dose ($p = 0.025$).

mechanism of NP toxicity, the alkaline comet assay was performed both with and without treatment with formamidopyrimidine DNA glycosylase (FPG). The addition of FPG allows the detection of oxidized purines, such as 8-oxoguanine, in addition to alkali-labile sites and single- and double-strand DNA breaks (SSB and DSB). Possible interference of SNPs with the enzymatic activity of FPG was tested in a preliminary experiment in which A549 cells were exposed to H_2O_2 and thereafter treated with the FPG enzyme pre-incubated with different concentrations of SNPs. No interaction between FPG and the SNPs was observed (data not shown). The alkaline comet assay was performed on cells treated for 15 minutes and 4 h with two doses (40 and 60 μg/ml) of 16 or 60 nm SNPs. H_2O_2 was used as a positive control. 16 nm and 60 nm SNPs were selected because of their apparently higher potential of MN induction. The 15-min time point was based on previous work on particle induction of oxidative damage (Lombaert et al. 2008). After this short period, no significant endogenous repair activity is expected. Treatment with 16 nm or 60 nm SNPs showed no increase of DNA strand breaks (or alkali-labile sites) after 15 min or 4 h as compared to the controls in the alkaline comet assay in absence of FPG (Figure 5). After FPG enzymatic treatment, a small but not statistically significant effect of SNPs was noted (Figure 5). The highest increase was observed after treatment with 60 μg/ml of S-60 SNPs for both time points. No consistent relationship with cellular dose, cell-associated particle number and cell-associated surface area was found (data not shown). These data suggested that only a minor fraction of the micronuclei observed in previous experiments may originate from oxidative damage resulting in double strand

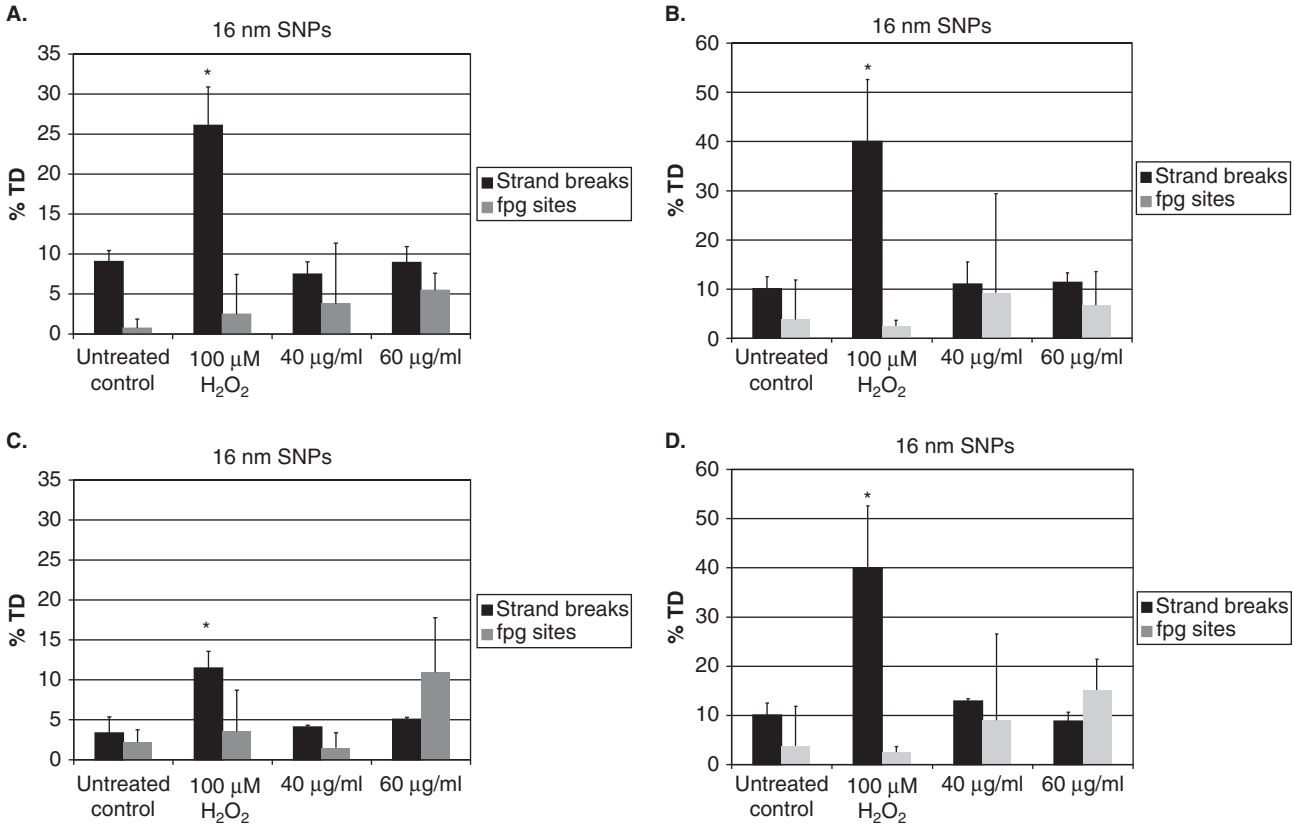

Figure 5. DNA strand breaks and FPG sensitive sites, expressed as % of tail DNA (% TD), in A549 cells following 15 min (A, C) and 4 h (B, D) of incubation with either 16 nm SNPs (A, B) or 60 nm SNPs (C, D). 100 μM H_2O_2 was used as positive control. Values are shown as mean ± SD of two experiments. *denote statistically significant differences ($p < 0.05$) compared to untreated controls as assessed by ANOVA analysis for either DNA single strand breaks or FPG sites.

DNA breaks and thus in acentric chromosome fragments.

Assessment of aneugenic versus clastogenic events

To analyze the possible induction of specific aneugenic and/or clastogenic events, the CBMN assay was performed in combination with pan-centromeric FISH after treatment with 16 and 60 nm SNPs. This allows discrimination between clastogenic (acentric chromosome fragments) and aneugenic (chromosome loss) effects and possibly a more sensitive detection of mutagenic effects. The same SNPs were selected as those tested previously. Nocodazole (0.02 μg/ml), a potent aneugen, was used as a positive control. The slight increase of MNBNs in cells treated with SNPs was confirmed although the size-dependent difference was less pronounced, probably due to the difficulty of discriminating binucleates from mononucleates with this type of staining (Figure 6). In addition, the comparison of centromere-positive (C+ MN) versus centromere-negative (C− MN) MN demonstrated a slight increase in the percentage of C+ MN. When considering the cellular mass, cell-associated particle number and cell-associated surface area doses, the percentage of C+ MN increased as a function of the cell-associated particle number and cell-associated surface area but not in function of the cellular mass dose (data not shown).

Mitotic arrest

Considering that the slight increase of MNMONO and induction of centromere-positive MN may indicate some interference with spindle microtubules, we decided to investigate whether other abnormal mitotic events, such as blockage of metaphase were induced by the SNPs. To assess the induction of metaphase block, mitotic indices were determined. Results (Supplementary data, Figure 2, available online) showed a decrease in mitotic index at the

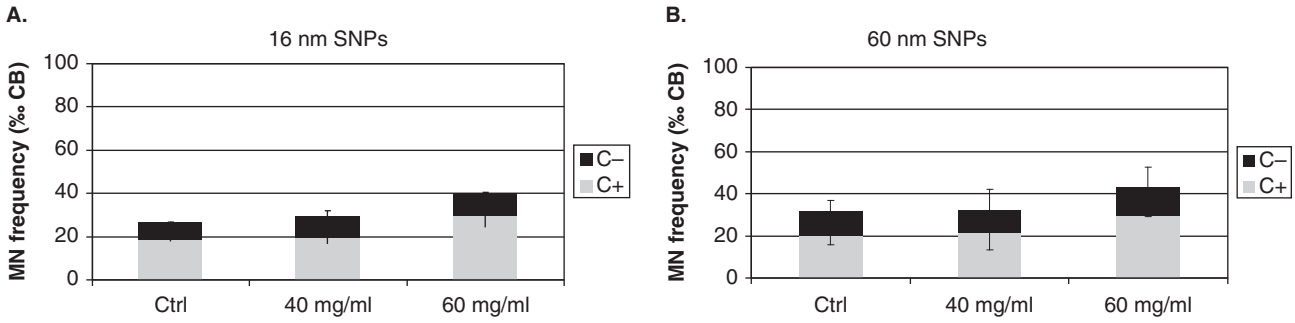

Figure 6. Frequency of centromere-positive (C+) and centromere-negative (C−) MNBN induced after 40 h treatment of A549 cells with 16 nm (A) and 60 nm (B) SNPs. 0.02 μM nocodazole (positive control) yielded an average of 193 MNBN/1000 BN scored with 75 ± 13% C+ MN. Values are shown as mean ± SD of two experiments. No statistically significant difference was observed compared to untreated controls after ANOVA analysis for the % C+ MNBN, % C− MNBN and total frequency of MNBN.

lower doses (10–20 μg/ml and 40–100 μg/ml for 60 and 104 nm SNPs, respectively) and an increased mitotic index at higher doses (40–60 μg/ml and 200–300 μg/ml for 60 and 104 nm SNPs, respectively), whereas this was less clear for A549 cells treated with the smallest SNPs (16 nm). The decrease in mitotic index may reflect a delay in mitosis at the lower doses whereas at higher doses of SNPs cells may be blocked in metaphase.

Chromosome loss, metaphase block and mitotic slippage are consequences of spindle defects. From a mechanistic point of view, it is considered that at individual cell level chromosome loss corresponds to the inactivation of a restricted number of tubulin fibers but that metaphase block results from a complete spindle disturbance; mitotic slippage being a possible exit for the latter. Figure 7 shows the total frequency of mitotic errors (mitotic arrest, mitotic slippage and chromosome loss) for the 16 and 60 nm SNPs for which FISH data were available.

An apparent effect of the nominal dose on the total number of mitotic abnormalities, although in different proportions, was observed for both SNPs. When considering the cellular doses, a trend towards increased abnormal mitotic events was observed with the appearance of metaphase block only at the highest concentrations. However, no consistent relationship was observed when abnormal mitotic events were expressed as a function of the cell-associated particle number or cell-associated surface area doses (data not shown).

Discussion

The size-effect of insoluble particles on cell toxicity and genotoxicity has been addressed by focusing essentially on the difference between nano- and micrometer size. Karlsson et al. (2009) demonstrated that for different endpoints such as cell toxicity and DNA damage nano-size metallic particles do not necessarily induce a stronger response as compared to their micrometer counterparts.

To assess the potential effect of nanosize on the genotoxicity of SNPs, we selected on the basis of earlier toxicity studies (Lison et al. 2008; Napierska et al. 2009) monodisperse amorphous Stöber silica particles of three different sizes within the nanoscale (16, 60 and 104 nm) and applied the *in vitro* cytochalasin-B micronucleus assay, a well validated genotoxicity assay capable of detecting both clastogenic and aneugenic effects. We selected a protocol of exposure with cytochalasin-B addition 4 h after the start of the treatment to minimize a potential interaction of cytochalasin-B on the early uptake of the particles. Two possible mechanisms of action were further explored with additional experiments, suggesting a weak induction of oxidative DNA damage (alkaline comet assay ± FPG), chromosome breakage and chromosome loss (FISH with pancentromeric probes). The latter which might be indicative of interference with the spindle was supported in part by monitoring mitotic arrest and mitotic slippage. All experiments were performed according to international guidelines available for the procedure and adapted for NPs, if required. Data results are from two repeat experiments with duplicate cultures. The physico-chemical properties of SNPs were well characterized. DLS measurements showed that protein binding, but no aggregation occurred. For the smallest particles with a diameter of 16 nm, this protein layer might lead to flocculation. Recently, Lundqvist et al. (2008) have demonstrated that depending on nanoparticle size and surface properties, the composition of the protein layer surrounding polystyrene nanoparticles differs. One can also not exclude that during cell culture, the SNPs get surrounded by a particular combination of biomolecules (proteins,

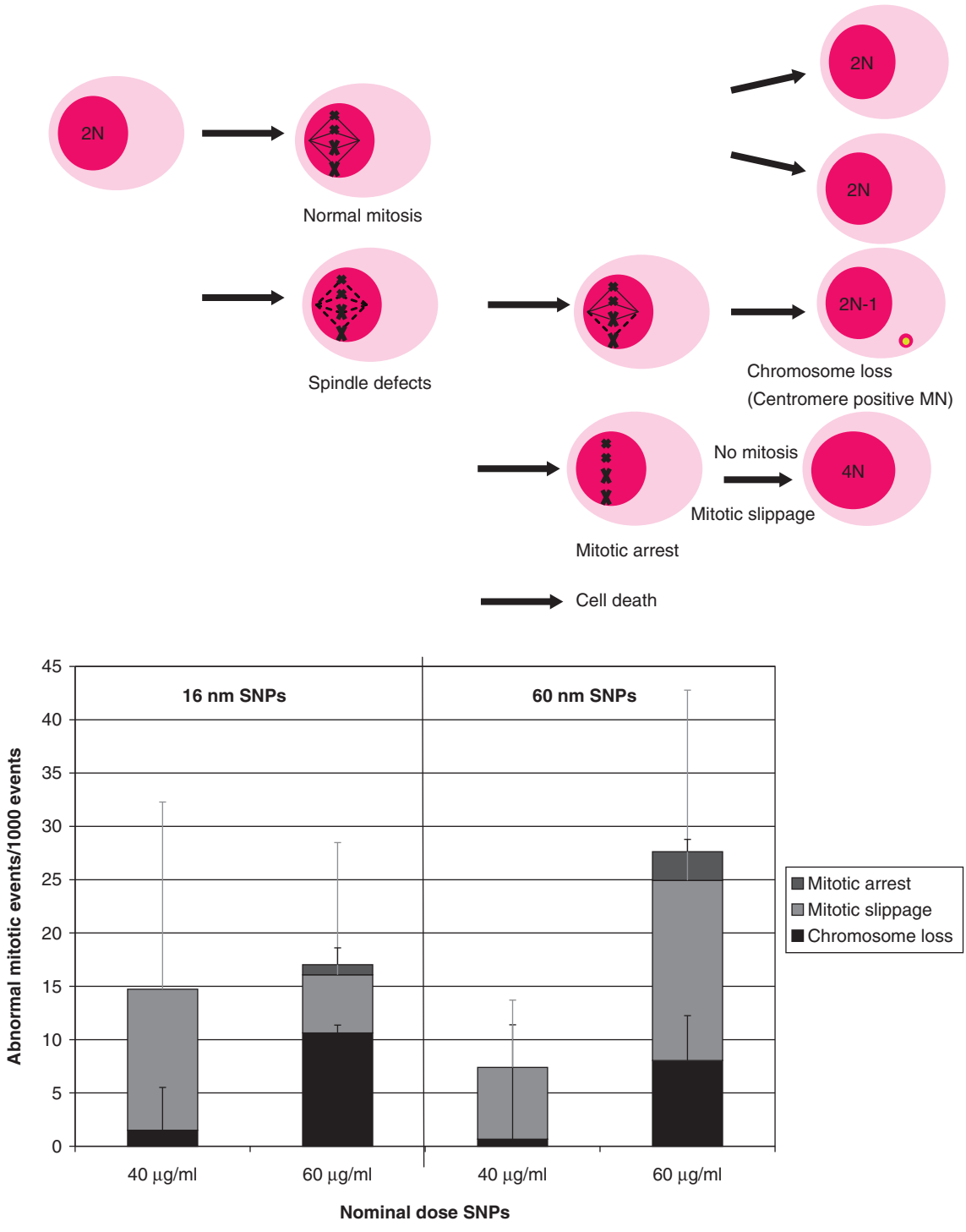

Figure 7. Frequency of mitotic errors (‰ cells) in A549 cells treated with 16 nm SNPs and 60 nm SNPs. Mitotic arrest and mitotic slippage were scored in the CBMN assay; chromosome loss corresponds to the centromere-positive micronuclei in the FISH CBMN assay. Control values are subtracted from the treatment, so untreated control values are equal to zero. No statistically significant difference was observed compared to untreated controls after ANOVA analysis for the frequency of mitotic errors (‰ cells).

etc.) which modulate the genotoxicity. The kinetics of cellular uptake was determined to allow the expression of the results as a function of the nominal or the cell-associated dose.

Our data indicate that, under these conditions, amorphous SNPs induced non-statistically significant genotoxic effects. The 16 nm particles showed an apparently higher fold induction of MNBN

compared to the 60 and 104 nm SNPs, possibly indicative of a size-dependent effect. Our MNBN data complement previous publications (Jin et al. 2007; Barnes et al. 2008; Park et al. 2009). Assessment of the (geno-) toxic effects of amorphous SNPs on A549 human lung epithelial carcinoma cells (50 nm SNPs) and 3T3-L1 fibroblasts (20–240 nm) revealed no genotoxicity as assessed by alkaline comet assay (Jin et al. 2007; Barnes et al. 2008). In contrast, Park et al. (2009) did observe adverse effects below cytotoxic concentrations by commercial Stöber SNPs (10–400 nm) in the embryonic stem cell test. They demonstrated the inhibition of stem cell differentiation towards myocardial cells after treatment with the smaller (10 and 30 nm) SNPs.

As far as other NPs are concerned, *in vitro* induction of MNBN has previously been observed for different NP types, such as carbon-based nanomaterials (Niwa and Iwai 2006; Muller et al. 2008), CoCr nanoparticles (Papageorgiou et al. 2007), titanium dioxide (Rahman et al. 2002; Gurr et al. 2005; Wang et al. 2007a) and crystalline silica (Wang et al. 2007b). Therefore the CBMN assay should be considered as an essential part of the test battery for assessment of NP genotoxicity. However, no definitive conclusions regarding the physico-chemical determinants of MN induction could be drawn from the previous data (Gonzalez et al. 2008). Additional studies with other particles performed in agreement with adapted guidelines and integrating findings on specific SNPs modes of action are required before establishing a definitive protocol. In particular the fact that cytochalasin-B should be added after the start of the treatment to avoid potential interaction between SNPs and the cytochalasin-B should be further documented (Doak et al. 2009).

For the assessment of insoluble particles our results suggest that both the nominal and the cellular dose should be considered depending on the target which is involved (cell membrane or intracellular structures). Therefore, the use of silica was a major advantage here since a quantitative measurement could be performed with high sensitivity and specificity. We already demonstrated that for cell toxicity assays (MTT, LDH and crystal violet) the nominal dose was an appropriate metric (Lison et al. 2008). Here, nominal or cell-associated particle number and nominal or cell-associated surface area doses were shown to correlate in a statistically significant way with the fold induction of MNBN when considering all tested SNPs together. The finding that both particle number and surface area accounted for MNBN induction, together with the observation that nominal and cellular dose demonstrated the same relationship with fold MNBN induction might have implications on the design of genotoxicity testing of nanomaterials. It should, however, be noted that we could not discriminate between particle-effect and dose-effects, because different doses were selected *a priori*. Particle size might not be critical for the actual induction of MNBN, but for reaching the cellular targets after endocytosis.

Results from complementary, more specific approaches suggest that SNPs may be capable of inducing slight chromosome breakage, loss and mitotic slippage, and at higher concentration possibly mitotic arrest. Since the dose-response relationship for MN (centromere positive) induction by tubulin inhibitors is known to be very steep and thresholded (Elhajouji et al. 1995, 1997; Kirsch-Volders et al. 2000), it is not surprising that dose-dependent relationships for mixed effects are not easily identified. Indeed the total MN frequency integrates the efficacy of inducing partial tubulin inactivation (chromosome loss as MN), absence of mitotic machinery (no production of MN due to mitotic block) followed or not by mitotic slippage (MN in polyploid mononucleates), the induction of double strand chromosome breakage (acentric fragments as MN) and cell death of micronucleated cells (not scored). To the best of our knowledge, our study is the first to suggest that non-cytotoxic doses of amorphous monodisperse silica nanoparticles may induce abnormal mitotic events such as chromosome loss and metaphase block. The latter was induced when higher doses of SNPs were added to the cell cultures, whereas at lower doses the mitotic activity decreased, possibly reflecting mitotic delay. It is highly probable that these aneugenic events result from spindle defects, and in particular interference with tubulin polymerization. Mechanical arguments are suggestive for this explanation since the smaller SNPs we used have almost the same size as the tubulin monomers. However, conclusive proof for the tubulin hypothesis requires additional work to demonstrate that they are effective targets. Besides chromosome loss, the studied SNPs induced some acentric fragments (centromere-negative MN). These might originate from ROS production but, contrary to Eom and Choi (2009), we did not find strong experimental support for this hypothesis (see Schins and Knaapen 2007) when considering non-cytotoxic doses of SNPs.

The results and conclusion presented here are relevant only for the tested monodisperse SNPs and for this cell line. Whether they are applicable to aggregated SNPs is another issue which deserves a systematic approach similar to this performed for the monodisperse SNPs.

In summary an appropriate evaluation of genotoxic effects induced by nanosize particles should not be restricted to nominal/cellular mass dose but include

particle number and surface area. With our exploratory approach aiming at covering a broad spectrum of genotoxicity related endpoints with different specificities and sensitivities, we found that non-cytotoxic doses of SNPs can induce some micronuclei but limited within a non-statistically significant range. In addition, weak effects such as chromosome damage, chromosome malsegregation and modulation of progression through mitosis were observed, but again without reaching statistical significance. It is possible that using more sensitive cell lines (e.g., p53 deficient cell lines) and/or tests optimized for evaluation of NPs, may lead to statistical significance. Although the precise mechanism as to how SNPs might function to perturb mitosis remains to be elucidated, it is well established that interference with the mitotic machinery leading to mitotic catastrophe and/or chromosome segregation errors can introduce multiple genetic alterations simultaneously and act as a driving force in tumorigenesis and acquisition of a malignant phenotype (Dey 2004; Kops et al. 2005).

Funding: This work was supported by the Belgian Ministry of Scientific Policy in the frame of the ''Science for sustainable development'' programme [SD/HE/02A].

Declaration of interest: The authors report no conflicts of interest. The authors alone are responsible for the content and writing of the paper.

References

Barnes CA, Elsaesser A, Arkusz J, Smok A, Palus J, Lesniak A, Salvati A, Hanrahan JP, Jong WH, Dziubaltowska E, Stepnik M, Rydzynski K, McKerr G, Lynch I, Dawson KA, Howard CV. 2008. Reproducible comet assay of amorphous silica nanoparticles detects no genotoxicity. Nano Lett 8(9):3069–3074.

De Boeck M, Lison D, Kirsch-Volders M. 1998. Evaluation of the in vitro direct and indirect genotoxic effects of cobalt compounds using the alkaline comet assay. Influence of interdonor and interexperimental variability. Carcinogenesis 19(11): 2021–2029.

De Boeck M, Lombaert N, De Backer S, Finsy R, Lison D, Kirsch-Volders M. 2003. In vitro genotoxic effects of different combinations of cobalt and metallic carbide particles. Mutagenesis 18(2):177–186.

Decordier I, Cundari E, Kirsch-Volders M. 2008. Mitotic checkpoints and the maintenance of the chromosome karyotype. Mutat Res 651(1–2):3–13.

Decordier I, De Bont K, De Bock K, Mateuca R, Roelants M, Ciardelli R, Haumont D, Knudsen LE, Kirsch-Volders M. 2007. Genetic susceptibility of newborn daughters to oxidative stress. Toxicol Lett 172(1–2):68–84.

Dey P. 2004. Aneuploidy and malignancy: An unsolved equation. J Clin Pathol 57(12):1245–1249.

Doak SH, Griffiths SM, Manshian B, Singh N, Williams PM, Brown AP, Jenkins GJ. 2009. Confounding experimental considerations in nanogenotoxicology. Mutagenesis 24(4):285–293.

Elhajouji A, Van Hummelen P, Kirsch-Volders M. 1995. Indications for a threshold of chemically-induced aneuploidy in vitro in human lymphocytes. Environ Mol Mutagen 26(4):292–304.

Elhajouji A, Tibaldi F, Kirsch-Volders M. 1997. Indication for thresholds of chromosome non-disjunction versus chromosome lagging induced by spindle inhibitors in vitro in human lymphocytes. Mutagenesis 12(3):133–140.

Elhajouji A, Cunha M, Kirsch-Volders M. 1998. Spindle poisons can induce polyploidy by mitotic slippage and micronucleate mononucleates in the cytokinesis-block assay. Mutagenesis 13(2):193–198.

Eom HJ, Choi J. 2009. Oxidative stress of silica nanoparticles in human bronchial epithelial cell, Beas-2B. Toxicol In Vitro 23(7):1326–1332.

Fenech M, Chang WP, Kirsch-Volders M, Holland N, Bonassi S, Zeiger E. 2003. HUMN project: Detailed description of the scoring criteria for the cytokinesis-block micronucleus assay using isolated human lymphocyte cultures. Mutat Res 534(1–2): 65–75.

Gonzalez L, Lison D, Kirsch-Volders M. 2008. Genotoxicity of engineered nanomaterials: A critical review. Nanotoxicology 2(4):252–273.

Gurr JR, Wang AS, Chen CH, Jan KY. 2005. Ultrafine titanium dioxide particles in the absence of photoactivation can induce oxidative damage to human bronchial epithelial cells. Toxicology 213(1–2):66–73.

Hoppe FM. 1993. Multiple comparisons, selection, and applications in biometry. New York: Marcel Dekker, Inc; 558 p.

International Agency for Research on Cancer (IARC). 1997. IARC monograph Vol. 68.

Jin Y, Kannan S, Wu M, Zhao JX. 2007. Toxicity of luminescent silica nanoparticles to living cells. Chem Res Toxicol 20(8):1126–1133.

Johansson C, Møller P, Forchhammer L, Loft S, Godschalk RW, Langie SA, Lumeij S, Jones GD, Kwok RW, Azqueta A, Phillips DH, Sozeri O, Routledge MN, Charlton AJ, Riso P, Porrini M, Allione A, Matullo G, Palus J, Stepnik M, Collins AR, Möller L. 2010. An ECVAG trial on assessment of oxidative damage to DNA measured by the comet assay. Mutagenesis 25(2):125–132.

Karlsson HL, Gustafsson J, Cronholm P, Møller L. 2009. Size-dependent toxicity of metal oxide particles – a comparison between nano- and micrometer size. Toxicol Lett 188(2): 112–118.

Kirsch-Volders M, Aardema M. Elhajouji A. 2000. Concepts of threshold in mutagenesis and carcinogenesis. Mutat Res 464(1):3–11.

Kirsch-Volders M, Fenech M. 2001. Inclusion of micronuclei in non-divided mononuclear lymphocytes and necrosis/apoptosis may provide a more comprehensive cytokinesis block micronucleus assay for biomonitoring purposes. Mutagenesis 16(1):51–58.

Kirsch-Volders M, Sofuni T, Aardema M, Albertini S, Eastmond D, Fenech M, Ishidate M Jr, Kirchner S, Lorge E, Morita T, Norppa H, Surralles J, Vanhauwaert A, Wakata A. 2003. Report from the in vitro micronucleus assay working group. Mutat Res 540(2):153–163.

Kirsch-Volders M, Sofuni T, Aardema M, Albertini S, Eastmond D, Fenech M, Ishidate M Jr, Kirchner S, Lorge E, Morita T, Norppa H, Surralles J, Vanhauwaert A, Wakata A. 2004. Corrigendum to "Report from the in vitro micronucleus assay working group". Mutat Res 564(1):97–100.

Kops GJ, Weaver BA, Cleveland DW. 2005. On the road to cancer: Aneuploidy and the mitotic checkpoint. Nat Rev Cancer 5(10):773–785.

Landsiedel R, Kapp MD, Schulz M, Wiench K, Oesch F. 2009. Genotoxicity investigations on nanomaterials: Methods, preparation and characterization of test material, potential artifacts and limitations – many questions, some answers. Mutat Res 681(2–3):241–258.

Lison D, Thomassen LC, Rabolli V, Gonzalez L, Napierska D, Seo JW, Kirsch-Volders M, Hoet PH, Kirschhock CE, Martens JA. 2008. Nominal and effective dosimetry of silica nanoparticles in cytotoxicity assays. Toxicol Sci 104(1): 155–162.

Lombaert N, Lison D, Van Hummelen P, Kirsch-Volders M. 2008. In vitro expression of hard metal dust (WC-Co) – responsive genes in human peripheral blood mononucleated cells. Toxicol Appl Pharmacol 227(2):299–312.

Lundqvist M, Stigler J, Elia G, Lynch I, Cedervall T, Dawson KA. 2008. Nanoparticle size and surface properties determine the protein corona with possible implications for biological impacts. Proc Natl Acad Sci USA 105(38):14265–14270.

Merget R, Bauer T, Kupper HU, Philippou S, Bauer HD, Breitstadt R, Bruening T. 2002. Health hazards due to the inhalation of amorphous silica. Arch Toxicol 75(11–12): 625–634.

Møller P, Möller L, Godschalk RW, Jones GD. 2010. Assessment and reduction of comet assay variation in relation to DNA damage: Studies from the European Comet Assay Validation Group. Mutagenesis 25(2):109–111.

Muller J, Decordier I, Hoet PH, Lombaert N, Thomassen L, Huaux F, Lison D, Kirsch-Volders M. 2008. Clastogenic and aneugenic effects of multi-wall carbon nanotubes in epithelial cells. Carcinogenesis 29(2):427–433.

Napierska D, Thomassen LC, Rabolli V, Lison D, Gonzalez L, Kirsch-Volders M, Martens JA, Hoet PH. 2009. Size-dependent cytotoxicity of monodisperse silica nanoparticles in human endothelial cells. Small 5(7):846–853.

Niwa Y, Iwai N. 2006. Genotoxicity in cell lines induced by chronic exposure to water-soluble fullerenes using micronucleus test. Environ Health Prevent Med 11:292–297.

Oberdörster G, Oberdörster E, Oberdörster J. 2007. Concepts of nanoparticle dose metric and response metric. Environ Health Perspect 115(6):290.

Organization for Economic Co-operation and Development (OECD). 2008. Guideline for the Testing of Chemicals: (Draft-Test Guideline 487).

Papageorgiou I, Brown C, Schins R, Singh S, Newson R, Davis S, Fisher J, Ingham E, Case CP. 2007. The effect of nano- and micron-sized particles of cobalt-chromium alloy on human fibroblasts in vitro. Biomaterials 28(19):2946–2958.

Park MV, Annema W, Salvati A, Lesniak A, Elsaesser A, Barnes C, McKerr G, Howard CV, Lynch I, Dawson KA, Piersma AH, de Jong WH. 2009. In vitro developmental toxicity test detects inhibition of stem cell differentiation by silica nanoparticles. Toxicol Appl Pharmacol 240(1):108–116.

Pluskota-Karwatka D. 2008. Modifications of nucleosides by endogenous mutagens-DNA adducts arising from cellular processes. Bioorg Chem 36(4):198–213.

Rahman Q, Lohani M, Dopp E, Pemsel H, Jonas L, Weiss DG, Schiffmann D. 2002. Evidence that ultrafine titanium dioxide induces micronuclei and apoptosis in Syrian hamster embryo fibroblasts. Environ Health Perspect 110(8):797–800.

Schins RP, Knaapen AM. 2007. Genotoxicity of poorly soluble particles. Inhal Toxicol 19(Suppl. 1):189–198.

Stoeger T, Schmid O, Takenaka S, Schulz H. 2007. Inflammatory response to TiO_2 and carbonaceous particles scales best with BET surface area. Environ Health Perspect 115(6):290–291.

Teeguarden JG, Hinderliter PM, Orr G, Thrall BD, Pounds JG. 2007. Particokinetics in vitro: Dosimetry considerations for in vitro nanoparticle toxicity assessments. Toxicol Sci 95(2):300–312.

Thomassen LC, Aerts A, Rabolli V, Lison D, Kirsch-Volders M, Gonzalez L, Napierska D, Hoet PH, Kirschhock CE, Martens JA. 2010. Synthesis and characterization of stable monodisperse silica nanoparticle sols for in vitro cytotoxicity testing. Langmuir 26(1):328–335.

Wang JJ, Sanderson BJ, Wang H. 2007a. Cyto- and genotoxicity of ultrafine TiO_2 particles in cultured human lymphoblastoid cells. Mutat Res 628(2):99–106.

Wang JJ, Sanderson BJ, Wang H. 2007b. Cytotoxicity and genotoxicity of ultrafine crystalline SiO2 particulate in cultured human lymphoblastoid cells. Environ Mol Mutagen 48(2):151–157.

Wittmaack K. 2007. In search of the most relevant parameter for quantifying lung inflammatory response to nanoparticle exposure: Particle number, surface area, or what? Environ Health Perspect 115(2):187–194.

Yang H, Liu C, Yang D, Zhang H, Xi Z. 2009. Comparative study of cytotoxicity, oxidative stress and genotoxicity induced by four typical nanomaterials: The role of particle size, shape and composition. J Appl Toxicol 29(1):69–78.

Zhang LW, Monteiro-Riviere NA. 2009. Mechanisms of quantum dot nanoparticle cellular uptake. Toxicol Sci 110(1):138–155.

Supplementary material available online

Supplementary Figures 1 and 2